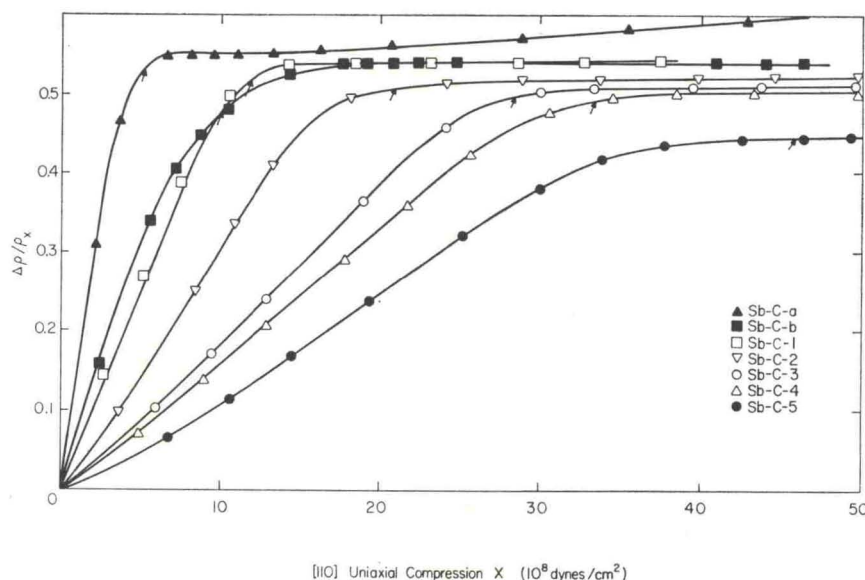


FIG. 2. Longitudinal piezoresistance as a function of [110] compressional stress (arrangement C) at 1.2°K for Sb-doped germanium. The arrows indicate the stress at which saturation is expected for parabolic bands.



ments the samples were about 0.8 cm long, 0.3 cm high (stress direction) and 0.1 cm thick. The two critical surfaces were polished flat and parallel, and the sample was then exposed to a fast, nonpreferential CP4 etch to remove surface damage.

III. EXPERIMENTAL RESULTS AND DISCUSSION

The samples are listed in Table I. The antimony concentration was obtained from Hall measurements at 300°K or 78°K, using $R = (en)^{-1}$. In some cases the Hall coefficient R differed by a few percent at these two temperatures. The R value of smallest magnitude was then used for the calculation of the concentration N . The uncertainty in N is approximately $\pm 3\%$.

The letters C , F , G , and H in the sample notation symbolize the various stress and current orientations as explained in Table II. This table also lists the energy shifts of the valleys caused by the shear part of the uniaxial compression X and the mobility components of the various valleys in the current direction. A shear

deformation potential $E_2 = 19$ eV/strain as obtained¹⁵ from lightly doped samples and the elastic shear constant¹⁶ $S_{44} = 1.47 \times 10^{-12}$ cm²/dyn will be used in the following.

Figures 2, 3, and 4 show the relative change of the resistivity $(\rho_x - \rho_0)/\rho_x$ as a function of compressional stress X at 1.2°K for the two longitudinal cases C and F and for the transverse case G , respectively. In the absence of any band tailing, which is expected to be caused by the random distribution of impurities, one expects these piezoresistance curves to saturate when all electrons are transferred from the higher valleys to the low valley or valleys. This should occur at a critical stress value⁶ for which the energy separation between the upper and lower valleys equals the Fermi energy of the lower valleys. For the cases C and F saturation occurs at stresses about 6×10^8 and 3×10^8 dyn/cm², respectively, higher than the theoretical value. Attributing this to tail states, one concludes that about 5% of the electrons are in states spread over 3 ± 1 meV below the band edge. A much smaller number of states which possibly are located further in the forbidden gap would not be detectable in this experiment.

In the transverse case G , the discrepancy between the experimental and theoretical saturation stress is as large as 25×10^8 dyn/cm². This is not a true effect but rather due to stress inhomogeneities which occur in the transverse stress arrangement. In order to obtain a homogeneous uniaxial compression the sample has to be free to expand sideways by an amount given by the Poisson ratio. In the longitudinal-stress measurements this condition is satisfied in the center region of the sample at distances from the sample mountings larger than $4w$, where w is the larger dimension perpendicular

TABLE II. Sample notation and mobility components for different orientations of compressional stress X and current I .

Sample notation	Orientation X	Orientation I	Shift of valleys ^a with respect to zero stress position	Mobility component in current direction
C	[110]	[110]	2 up $E_2 S_{44} X / 6$	μ_1
			2 down $-E_2 S_{44} X / 6$	$(\mu_1 + 2\mu_{11}) / 3$
F	[111]	[111]	3 up $E_2 S_{44} X / 9$	$(8\mu_1 + \mu_{11}) / 9$
			1 down $-E_2 S_{44} X / 3$	μ_{11}
G	[111]	[1 $\bar{1}0$]	3 up $E_2 S_{44} X / 9$	μ_1 (one)
			1 down $-E_2 S_{44} X / 3$	$(\mu_1 + 2\mu_{11}) / 3$ (two)
H	[110]	[001]	2 up $E_2 S_{44} X / 6$	$(2\mu_1 + \mu_{11}) / 3$
			2 down $-E_2 S_{44} X / 6$	$(2\mu_1 + \mu_{11}) / 3$

^a $E_2 = 19$ eV is the shear deformation potential; $S_{44} = 1.47 \times 10^{-12}$ cm²/dyn is the shear elastic constant.

¹⁵ H. Fritzsche, Phys. Rev. **115**, 336 (1959).

¹⁶ M. E. Fine, J. Appl. Phys. **24**, 338 (1953).

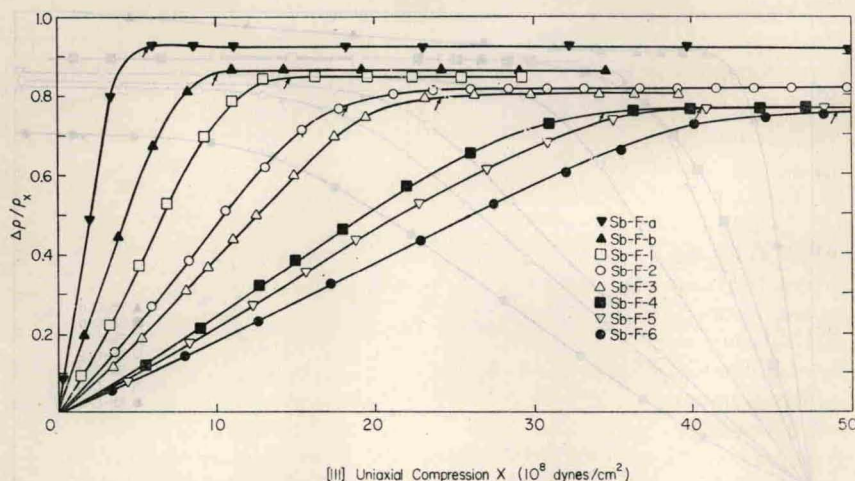


FIG. 3. Same as Fig. 2 for [111] compressional stress (arrangement *F*).

to the length of the sample. This condition is never satisfied in the transverse arrangement, however, since friction prevents the sample from expanding sideways at the surfaces where the compression is applied. In the Appendix, this case will be discussed in detail. It will be shown there that the piezoresistance at large stresses is not affected by the inhomogeneous stress distribution.

The piezoresistance of sample Sb-C-a shown in Fig. 2 appears to saturate near $X = 8 \times 10^8$ dyn/cm². It continues to rise, however, at larger stress values. The origin of this effect, which was only observed at the low-concentration end of the range investigated, is not yet understood. This sample is not used in our later analysis.

A. Saturation Values of the Piezoresistance

Most direct information can be obtained from the piezoresistance at stresses far beyond the saturation stress where one can safely assume that all electrons are transferred to the lowest valley or valleys. Under the assumption that the total carrier concentration is

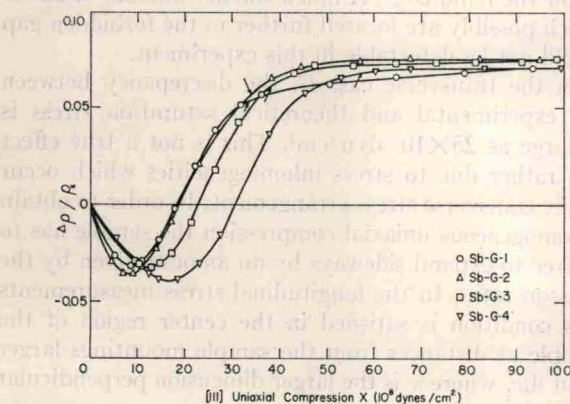


FIG. 4. Transverse piezoresistance as a function of [111] compressional stress (arrangement *G*) at 1.2°K for Sb-doped germanium. The arrows indicate the saturation stress for parabolic bands.

unchanged by the application of stress the principal mobility components, μ_{11} and μ_{\perp} can be determined from the saturation $\Delta\rho/\rho_x$ of case *F* and *G*, respectively, and the component $(\mu_{\perp} + 2\mu_{11})/3$ from that of case *C* (see Table II). The saturation values of $\Delta\rho/\rho_x$ remained constant at stresses above 5×10^9 dyn/cm². This region is not shown in Figs. 2 and 3.

The mobility components thus determined are plotted as a function of donor or carrier concentration in Fig. 5. Also included in that figure are previously measured data points¹⁷ of zero-stress mobility and μ_{11} of samples containing smaller N . The arrows at $N = 10^{17}$ cm⁻³ and $N = 2.1 \times 10^{17}$ cm⁻³ indicate the critical concentrations N_c for the transition¹⁸ from nonmetallic to metallic conduction for zero stress and case *F*, respectively, in Sb-doped germanium. This transition is usually defined as the concentration N_c at which the thermal activation energy ϵ_2 of impurity conduction¹⁷ vanishes. This happens when the ratio¹⁹ $r_s/a \approx 3.5$, where $r_s = (\frac{3}{4}\pi N)^{1/3}$ and a = effective Bohr radius. N_c is different for case $X = 0$ and case *F* because of the reduction of a by the [111] compressional stress.²⁰

It is remarkable that no break in the dependence of mobility on N accompanies the transition from nonmetallic to metallic conduction as defined in this way. The mobility, which increases rapidly with N below N_c because of the increasing overlap of the impurity wave functions continues to increase above N_c . After reaching a maximum value near $N = 10^{18}$ cm⁻³ for $X = 0$ and about about 3×10^{18} cm⁻³ for case *F*, the mobility decreases with increasing N . It is only in this higher concentration range that the mobility shows a behavior similar to an impure metal.

In the range $10^{17} \leq N \leq 10^{18}$ cm⁻³, Sb-doped Ge is metallic in the sense that the extrapolation of the resis-

¹⁷ H. Fritzsche, Phys. Chem. Solids 6, 69 (1958); Phys. Rev. 125, 1552 (1962).

¹⁸ N. F. Mott, Phil. Mag. 6, 287 (1961).

¹⁹ N. F. Mott and W. D. Twose, Phil. Mag. Suppl. 10, 107 (1961).

²⁰ H. Fritzsche, Phys. Rev. 125, 1560 (1962).